ChemComm

FEATURE ARTICLE

View Article Online
View Journal | View Issue

Cite this: *Chem. Commun.*, 2025, **61**, 441

Functional coordination compounds for mechanoresponsive polymers

Tatiana Gridneva and Julia R. Khusnutdinova *

Received 22nd October 2024,
Accepted 27th November 2024

DOI: 10.1039/d4cc05622a

rsc.li/chemcomm

Small molecule probes that respond to a mechanical force (''mechanophores'') have emerged as an important tool in the design of stimuli-responsive polymer materials. Although the majority of such mechanohphores are based on organic molecules, the utilization of metal complexes has also attracted attention as they offer a possibility to tune their spectroscopic properties and reactivity, and have the ability to reversibly form and break metal–ligand bonds through rational design of the ligand environment surrounding the metal. This review features representative examples of coordination compounds which were utilized as new, tunable tools to create various types of mechanoresponsive polymers.

Introduction

Mechanoresponsive materials have emerged as a class of stimuli-responsive materials which can change their properties (*e.g.* color, emission) in response to an applied mechanical force. Among them, mechanoresponsive polymers[1] are of particular interest due to the wide range of applications that span everything from everyday consumables and flexible medical devices to construction materials.

The most common strategy for the preparation of mechanoresponsive polymers is the incorporation of small molecules, ''mechanophores'', that respond to mechanical force. Mechanophores can be incorporated into polymers by either simple blending into the matrix or by covalent attachment to the polymer chains. Activation of a mechanophore by mechanical force typically results in changes at the molecular level (*e.g.* bond cleavage, dissociation of weak interactions, conformational change, *etc.*) which will then result in a measurable property change of the bulk material such as color changes, modification of the material's luminescence properties, the initiation of a chemical reaction, phase transition, *etc.*

Most commonly utilized mechanophores are small organic molecules, with many examples involving covalent bond-cleavage such as in spiropyran,[2] naphthopyran,[3] oxazine derivatives,[4] 1,2-dioxetane,[5] diaryldibenzofuranone,[6] Diels–Alder adducts,[7] and ladderanes.[8] Other examples involve more subtle changes in the chemical structure, for example, *via* disrupting aggregation behavior[9] or charge transfer pairs.[10] Furthermore, new types of mechanophores which can be activated by subtle conformational

Okinawa Institute of Science and Technology Graduate University, 1919-1 Tancha, Onna-son, Kunigami-gun, Okinawa, 904-0495, Japan. E-mail: juliak@oist.jp

Tatiana Gridneva

Tatiana Gridneva received her Bachelor's degree in Engineering from the Tokyo University of Agriculture and Technology in 2019, where she conducted research on ruthenium carbide carbonyl clusters under the supervision of Professor Masafumi Hirano. Currently she is a PhD student at the Coordination Chemistry and Catalysis Unit in Okinawa Institute of Science and Technology under the supervision of Professor Julia R. Khusnutdinova. Her research focuses on the study of mechanoresponsive polymers incorporating photoluminescent copper(I) complexes.

Julia R. Khusnutdinova

Julia Khusnutdinova is an associate professor at Okinawa Institute of Science and Technology (OIST) leading Coordination Chemistry and Catalysis Unit. Her main research interests include mechanoresponsive polymers, organometallic chemistry, and transition metal catalysis. She received her undergraduate degree at Kazan State University and completed her PhD degree at the University of Maryland in College Park, USA. Prior to OIST, she worked as a postdoctoral researcher at Washington University and at the Weizmann Institute of Science and Technology.

changes[11] have emerged recently, represented by the "flapping molecule" reported by Kotani *et al.*[11c] Apart from organic small molecules, diverse motifs such as *o*-carboranes,[12] proteins,[13] enzymes,[14] and DNA[15] were utilized as mechanophores.

Metal complexes, in which a weak metal–ligand bond is targeted for mechanocactivation, have been considered promising candidates for the design of mechanoresponsive polymers. The properties of coordination compounds and the strength of the metal–ligand bond can be tuned by the choice of the metal center, its oxidation state, and the ligand structure, providing flexibility in mechanophore modification. The cleavage of a dative bond of the coordination compound-based mechanophores can result in responses such as changes in the optical properties of the material, catalyst activation, metal ion release, and others (*vide infra*). Furthermore, recent studies have demonstrated that the combination of metal complexes with well-established, organic-based mechanophore systems can alter or enhance their properties; coordination with the activated mechanophore may induce charge transfer and other phenomena, opening up further possibilities in the application of previously developed materials. Finally, coordination compound-based mechanophores can find new activation pathways that are not observed in the classical organic-based mechanophores. For example, covalent bond cleavage often means there is a limited degree of reversibility, while metal–ligand bond cleavage is in many cases easily reversible, and this property can be used to obtain fast and reversible responses to mechanical force.

Since it was first demonstrated that ultrasonication or shearing force can cleave metal–ligand bonds in polymer chains in the early 2000s,[16] a number of mechanoresponsive systems utilizing coordination bond cleavage have been developed, although they generally received less attention than organic-based mechanophores and were not specifically reviewed in the literature. In this article, we will focus on the utilization of metal complexes in mechanoresponsive materials and highlight selected examples of mechanoresponsive polymer systems, where a coordination bond is involved in the mechanoresponse. The examples are categorized by the mechanism of the mechanophore activation: (1) cleavage of the metal–ligand bond; (2) interaction of metal species with organic mechanophores; and (3) metal complexes with conformationally labile ligands. This review does not aim to be a comprehensive description of all coordination compounds that act as mechanophores; its main goal is to illustrate a variety of application of coordination bonds in mechanoactivation.

Systems with mechanophores solely based on organic molecules will be not covered in this review since they are discussed in previous literature (*vide supra*).

Activation by cleavage of the metal–ligand bond

Metal–ligand bond cleavage upon mechanical force application, typically in polymers with covalently incorporated metal complexes containing weak bonds, is the most straightforward and widely used approach for the design of mechanophores. In this paper, representative examples of mechanophores activated by metal–ligand bond cleavage are introduced and divided into three sections: the cleavage of metal–ligand bonds to generate catalytically active species; the cleavage of sandwich complexes by force, and finally dynamic metal–ligand bonds.

Cleavage of metal–ligand bonds to generate catalytically active species

In this section, examples of the generation of the active catalysts from the latent pre-catalyst *via* mechanoactivation will be discussed, mostly limited to the metal complexes covalently attached to the polymer chain.

In 2008, Sijbesma and co-workers reported that a silver N-heterocyclic carbene (NHC) complex attached to a polymer chain can be cleaved by ultrasonication in solution, and the process can be monitored by the formation of the imidazolium product in the presence of water.[17] Based on these findings, the activation of a homogeneous catalyst induced by a mechanical force was later achieved by the same group.[18] Silver(I) complexes of NHCs functionalized with poly(tetrahydrofuran) (pTHF) were prepared (Fig. 1a), and sonication experiments together with benzyl alcohol and vinyl acetate were performed to study the activity of the complexes as latent catalysts for transesterification. Catalyst **1a** bearing ligands with a molecular weight of 5.0 kDa showed a turn-over number exceeding 800 and 65%

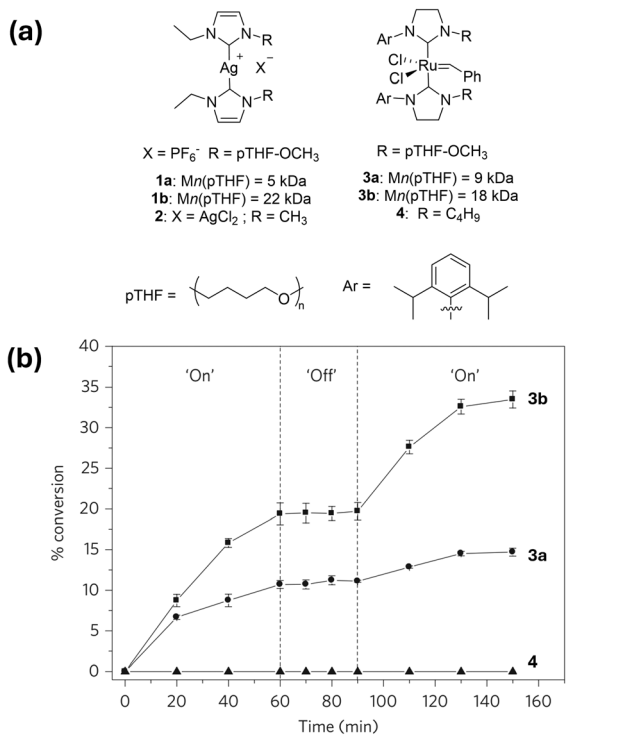

Fig. 1 (a) pTHF functionalized Ag^{I}–NHC complexes (**1a** and **1b**) and Ru^{II}–NHC complexes (**3a and 3b**) with corresponding non-polymeric analogues **2** and **4**. (b) Time–conversion plots of the sonication-induced RCM reaction of diethyl diallylmalonate at 20 °C using **3a**, **3b** and **4** as catalysts. Error bars are based on standard errors in duplicate runs. Image (b) is adapted with permission from ref. 18. Copyright 2009, Springer Nature.

conversion after 60 min of sonication. Sonication without the catalyst, on the other hand, did not yield the product.

Detailed mechanistic studies of bond scission in the Ag–NHC system reported later revealed that the activation *via* radical species can be excluded as predominant mechanisms for the activation of the latent catalyst.[19]

Using a similar approach, mechanoactivation of the ruthenium–alkylidene complexes was achieved to induce catalytic olefin metathesis reactions. The latent bis[*N*-(alkyl)-*N*-(2,6-diisopropylphenyl)carbene]Ru catalysts were activated by sonication to catalyze both a ring-closing metathesis (RCM) reaction of diethyl diallylmalonate and a ring-opening metathesis polymerization (ROMP) of cyclooctene. When a ligand with a short butane substituent (complex **4**, Fig. 1) was used instead of pTHF, no reactivity was observed for both RCM and ROMP reactions which supports the mechanical rather than thermal activation pathway for the catalyst at room temperature. Notably, when the sonication was interrupted during the RCM reaction, the conversion increase also stopped, indicating that the active catalyst species have a limited lifetime (Fig. 1b).

Further investigations of the Ru–NHC latent catalyst revealed that in the RCM reaction the lifetime of the active species can be increased by addition of triphenylphosphine or by increasing the substrate concentration. In the case of ROMP, the active species were found to have a lifetime of several hours.[20]

Later, Sijbesma and co-workers demonstrated that the activation of the latent catalyst is not limited to solution, but can also be achieved in the bulk material.[21] The polymer-functionalized ruthenium–alkylidene NHC catalyst discussed above was blended with the norbornene monomer in the pTHF matrix, and compression force was employed to activate the latent catalyst and promote the ROMP reaction (Fig. 2). During 5 cycles of 5 min compression for each cycle (with folding the sample in between compression cycles), the conversion of the polymerization reaction increased approximately linearly and finally reached 25% (average of multiple batches). The use of a bifunctional monomer resulted in a cross-linked product, demonstrating the potential application of the system to mechanosensitive self-healing polymer materials.

In 2015, Binder and Michael reported that the mechanical activation of the latent NHC catalyst can be expanded to the copper(I)-catalyzed azide–alkyne cycloaddition (CuAAC) click reaction by polymer-chain functionalized Cu–NHC complexes, both in solution and in bulk material (Fig. 3a).[22] In the case of activation in solution, $[Cu(polymer\text{-}NHC)_2]X$ (X = Br^-, I^-, PF_6^-) complexes were sonicated together with phenylacetylene and benzylazide. The click reaction was followed by NMR spectroscopy, with conversion of up to 44%. Notably, the catalyst **5b** bearing rigid poly(styrene) (PS) based ligands showed higher conversion compared to catalyst **5a** bearing poly(isobutylene) (PIB) chains, even in the case when the PIB catalyst with higher molecular weight ligands was employed. Moreover, the mechanical activation of the click reaction was demonstrated in bulk pTHF by compression. The latent catalyst **5a** was embedded into the polymer matrix together with phenylacetylene and 3-azido-7-hydroxycoumarin, and the formation of the fluorogenic 7-hydroxy-3-(4-phenyl-1*H*-[1,2,3]triazole-1-yl)-coumarin dye

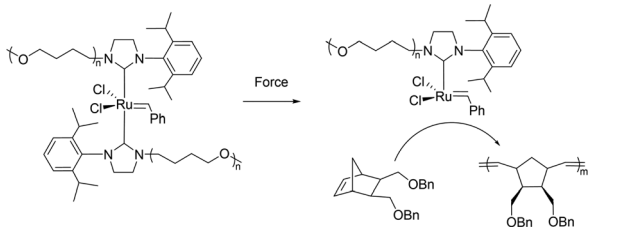

Fig. 2 Activation of the latent polymeric ruthenium–alkylidene NHC catalyst by compressive force and subsequent polymerization of the norbornene monomer. Scheme redrawn from ref. 21.

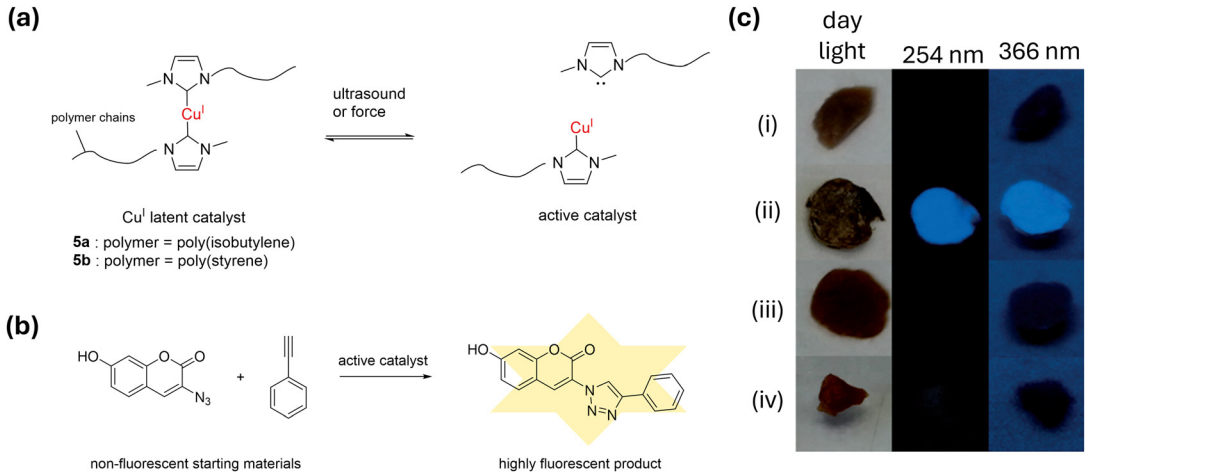

Fig. 3 (a) Structure of the latent Cu^I–NHC catalysts bearing PIB chains (**5a**: $M_{n(GPC)}$ = 4750–17 200 mol^{-1}) and PS chains (**5b**: $M_{n(GPC)}$ = 13 100 mol^{-1}), and their active form. (b) The click reaction of phenylacetylene and 3-azido-7-hydroxycoumarin catalyzed by the active Cu^I–NHC catalyst. (c) Photographs of the mechanochemical activation of the latent mechanocatalyst within the bulk material containing the starting materials. (i) Before compression with **5a**. (ii) After compression with **5a**. (iii) After compression without **5a**. (iv) With **5a**, without compression, after thermo-treatment at 60 °C. Scheme (a) and (b) are redrawn from ref. 22. Image (c) is adapted with permission from ref. 22. Copyright 2015, John Wiley and Sons.

by the click reaction enabled quantitative evaluation of the catalytic reaction (Fig. 3b). Upon application of 10 tons of pressure (3 × 30 min), an increase of blue fluorescence at 427 nm could be observed, indicating the successful mechanical activation of the catalyst (Fig. 3c). By fluorescence measurement after compression, the conversion of the reaction was calculated to be approximately (4.3 ± 1)%. In the case of control experiments without the mechanophore catalyst or with heating to 60 °C without compression, no significant fluorescence was observed.

Further investigation by the same group was conducted on the mechano-activated CuAAC click reaction by latent polymeric Cu^{I}–NHC catalysts. By employing polymers with different architectures (Fig. 4), it was found that sample **7** bearing the chain-extended structure and sample **8** bearing a cross-linked network structure are much more efficient in the CuAAC click reaction compared to the sample **6** bearing a single-unit linear polymer chains.[23] The Cu^{I}-bis(NHC) mechanophoric catalyst was also found to be highly adaptable towards incorporation into various motifs such as amino-acids,[24] peptides,[24,25] polyurethane thin films,[26] metal–organic frameworks,[27] and 3D-printed composites,[28] while preserving its mechanoresponsive properties.

Apart from metal–NHC complexes, mechanoactivation of latent catalysts has been reported in Pt–acetylide catalyzed olefin hydrosilylation by Wei *et al.* in 2017.[29] Poly(methyl-acrylate) (PMA) chains containing a Pt–acetylide complex in the center were prepared (Fig. 5a), and the scission at the Pt mechanophore under pulsed ultrasonication in solution was confirmed by gel permeation chromatography (GPC) and UV/Vis spectroscopy. In order to investigate the catalytic activity in olefin hydrosilylation, sonication of the solution containing the catalyst in a mixture with the substrate and reagent (1-octene

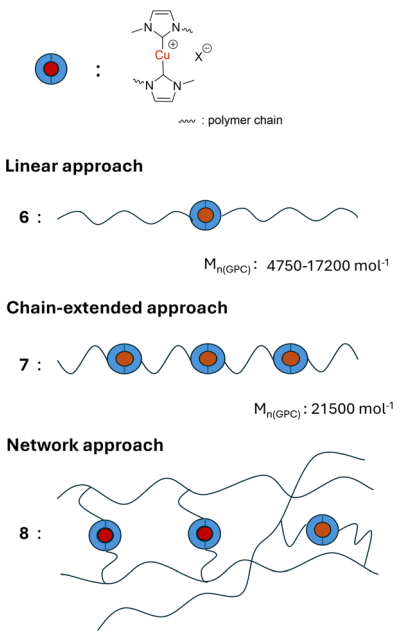

Fig. 4 Schematic illustration of polymers incorporating $[Cu(NHC)_2]X$ latent catalysts with different polymeric architectures. Figure redrawn from ref. 23.

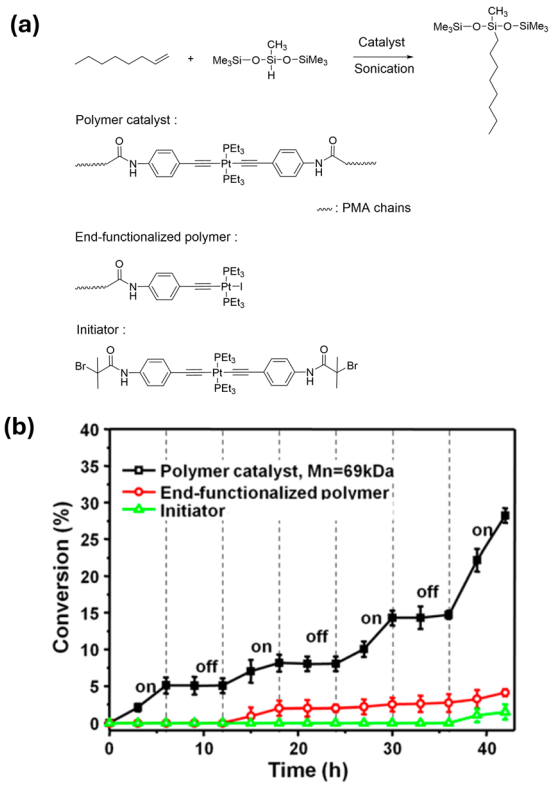

Fig. 5 (a) Scheme showing the mechanochemical regulated hydrosilylation of 1-octene by $(Me_3SiO)_2MeSiH$, and the structure of the Pt–acetylide polymer catalyst, end-functionalized polymer and the initiator. (b) Time–conversion plots of the hydrosilylation reaction catalyzed by the polymer catalyst, end-functionalized polymer, and initiator, respectively. Error bars are derived from standard errors in multiple runs. Image (b) is adapted with permission from ref. 29. Copyright 2017, American Chemical Society.

and $(Me_3SiO)_2MeSiH$) was performed. The reaction conversion showed an "on–off" behavior with no conversion observed during interruption of the sonication, indicating the short lifetime of the active species, similar to the Ag–NHC mechanocatalyst (Fig. 5b). The reaction conversion reached 28% after four 6 h periods of sonication, interrupted for three 6 h periods. In the case of a polymer bearing the Pt–acetylide complex at the end or the Pt–acetylide initiator not attached to a polymer chain, only very small conversions (<5%) were observed under the same conditions.

The cleavage of sandwich complexes by a mechanical force

Since their discovery in 1950s, ferrocene (Fc) and its analogue metallocenes have attracted much interest in various fields due to their unique structure and properties.[30] Although the cyclopentadienyl (Cp) moieties of metallocenes are known to rotate easily, making them applicable as rotamers, the metal–Cp bonds have very high dissociation energies sometimes even exceeding those of covalent C–C bonds (ex. 90 kcal mol^{-1} for Fc).[31]

However, recent studies showed that application of mechanical force to the polymer chains can lead to different reaction pathways and cleave the metallocene core, opening up the possibility of application of metallocenes as mechanophores.[32]

The cleavage of the metal–Cp bond can result in the release of Fe and Cp moieties, which can further react with the surrounding molecules and lead to a macroscopic response in the system. While there is often a trade-off between the thermal stability and mechanical lability in conventional mechanophores, metallocene-based mechanophores represent an example showing high force-free stability and high mechanical lability.

One of the first reports of an Fc derivative as a mechanophore in polymer chains which releases the metal ion on application of mechanical stress in solution was that by Giannantonio *et al.* in 2018.[33] PMA and polyurethane (PU) with Fc units attached to the main polymer chain through two Cps were prepared (**Fc–PMA** and **Fc–PU**, Fig. 6a). Upon ultrasonication, the number average molecular weight of **Fc–PMA** decreased much faster than that of the reference PMA without Fc units. Halving of the M_n was observed by size-exclusion chromatography, which indicated the preferential cleavage of the Fc units that are in the middle of the polymer chain. Furthermore, the addition of potassium thiocyanate to the sonicated solutions turned the solution of **Fc–PMA** red, characteristic of an iron(III) thiocyanate complex, indicating the release and oxidation of iron upon ultrasonication (Fig. 6b). In the case of **Fc–PU**, which has more Fc units per polymer chain, the formation of the red thiocyanate complex can be observed at lower concentrations of the polymer as compared to **Fc–PMA**. An application of the iron ion release was demonstrated by the formation of Prussian blue on sonication of **Fc–PU** in a solution of $K_4[Fe(CN)_6]$ (Fig. 5c).

Sha *et al.* independently demonstrated the preferential cleavage of the Fe–Cp bond of the Fc units incorporated in polybutadiene-like polymers by pulsed ultrasonication.[34] The sonication process was monitored by NMR with peaks of the dissociated Cp units (as cyclopentadiene attached to the polymer) generated during sonication. Successful detection of the iron ion by the phenanthroline ligand, the absence of radical species detected by TEMPO and finally computational studies utilizing the constrained geometries simulate external force (CoGEF) method all suggested a predominate heterolytic cleavage process of a Fc unit to Cp^- and $[CpFe]^+$ fragments, which is considered to follow further decomposition and H-atom abstraction (Fig. 7a).

Further publications from the same group demonstrated that ruthenocene and cobaltocenium derivatives in polymer chains can be similarly activated by mechanical force, although the parent sandwich complexes are even more inert than Fc.[35] Both were found to undergo heterolytic cleavage; however, the cleavage mechanisms different from Fc were suggested based on the CoGEF studies.

In the case of the ruthenocene mechanophore, it was suggested that the dissociation involves two steps in contrast to one step in the case of Fc, which can be attributed to a different coordination structure available in the case of ruthenium but not in the case of iron (Fig. 7b).[35a] On the other hand, in the case of cobaltocenium mechanophores, which are charged species, the computational studies suggest that during the elongation the counter-anion inserts between the two Cp rings, finally leading to the "peeling" dissociation of cobaltocenium in contrast to Fc where a "shearing" or "slipping" dissociation motion was observed.[35b]

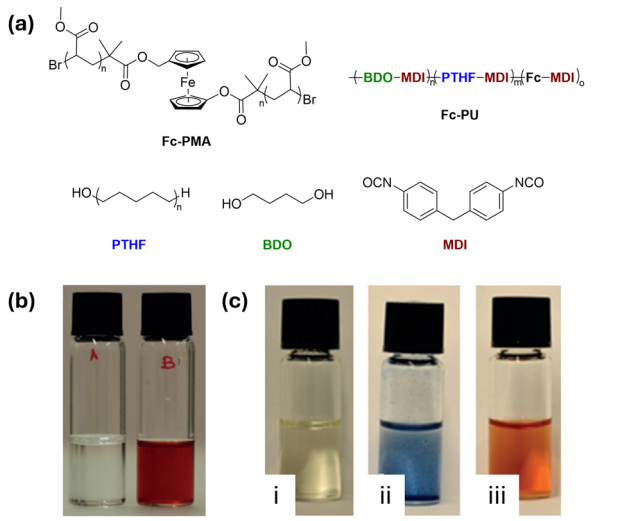

Fig. 6 (a) Structures of **Fc–PMA** and **Fc–PU**. (b) Solution of **Fc–PMA** with KSCN added before sonication (left) and after sonication (right). (c) Color change of the solution of **Fc–PU** (i) before sonication in the presence of $K_4[Fe(CN)_6]$, (ii) after sonication with $K_4[Fe(CN)_6]$, and (iii) after sonication with KSCN. Images (b) and (c) are adapted with permission from ref. 33. Copyright 2018, John Wiley and Sons.

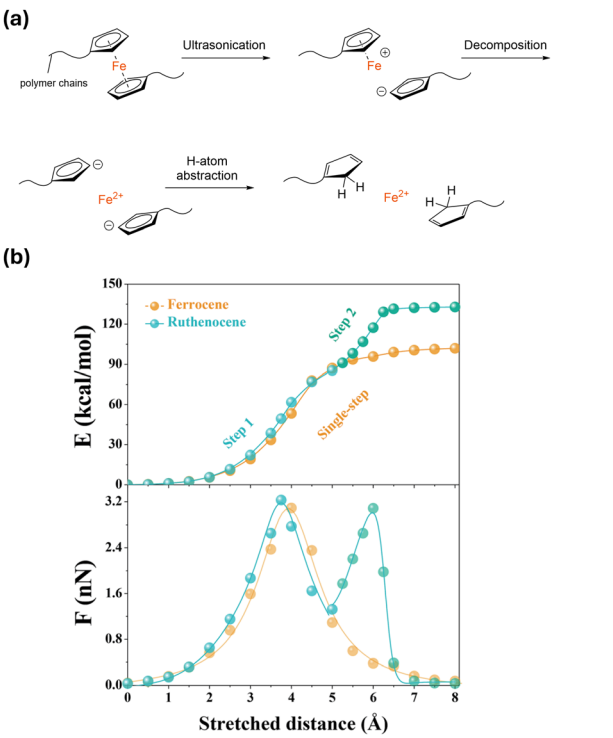

Fig. 7 (a) Proposed heterolytic dissociation mechanism of a Fc-containing polymer by ultrasound-induced chain scission. (b) CoGEF potential and force as a function of stretched distance for ruthenocene and Fc model compounds. Image (b) is reproduced with permission from ref. 35*a*. Copyright 2019, The Royal Society of Chemistry.

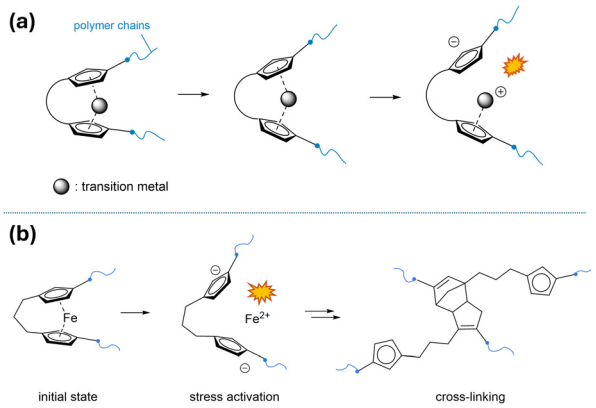

Fig. 8 (a) Schematic illustration of the proposed dissociation mechanism of mechanochemical "peeling" of conformationally locked metallocenophane. (b) Schematic illustration of the activation of ansa-ferrocene containing polymers by sonication followed by cross-linking *via* the Diels–Alder reaction (or dimerization) between Cp units. Figures redrawn from ref. 36.

In 2021, Zhang *et al.* reported that restricting the Cp rotation by bridging the two Cp components with a short alkyl chain can direct the mechanism of Fe–Cp mechanoactivation towards the "peeling" pathway instead of the shearing pathway (Fig. 8a).[36] Single-molecule force spectroscopy studies and computational analysis of polymer chains incorporating such ansa-ferrocenes demonstrated that restricting the conformational freedom of Fc and altering its dissociation pathway can lead to an altered mechanoinduced reactivity. The mechanoresponsive behavior of ansa-ferrocene mechanophores was tested in bulk silicone elastomers. The ansa-ferrocene mechanophores as well as normal Fc mechanophores were covalently incorporated as cross-linkers in the polymer network, and phenanthroline was introduced into the elastomers as an iron ion detector by swelling. A drop test and a split Hopkinson pressure bar test showed that in both cases the ansa-ferrocene sample developed a deeper red color after the impact compared to normal Fc. Furthermore, sonication of the ansa-ferrocene sample containing linear polymers resulted in an interesting application (dramatic mechanical change upon introduction of mechanical stress), where an insoluble cross-linked network formed due to the dimerization of the bridged Cp ligand after cleavage of the Fc moiety (Fig. 8b). As might be expected, in the case of normal Fc containing polymers no cross-linking was observed.

Labile metal complexes

In contrast to the irreversible metal–ligand bond cleavage highlighted in the previous sections, facile and usually reversible metal–ligand dissociation in labile metal complexes can afford responsive systems which are able to restore their initial properties on removal of the external stimulus, and are moreover able to report the strength of the stimuli by possessing a dynamic response.

The typical requirement for the coordination complex to exhibit dynamic reversibility is to have high thermodynamic stability and at the same time high kinetic lability.[37]

With the appropriate choice of a metal–ligand combination, polymers that are fully or partially connected by coordination bonds may allow for the controlled activation of the metal–ligand bonds when triggered by a stimulus. Indeed many examples showing thermo-, mechano-, chemo- and other stimuli-responsive properties have been reported.[38] Another specific feature of the metal-containing gels and polymers is the dependence of their properties on the oxidation state of the metal, which affects the stability and lability of metal complexes.[39] In this section, representative examples among mechanoresponsive polymers which utilize dynamic and reversible coordination bonds are highlighted.

In one of the early examples reported by Beck and Rowan in 2003,[16a] metallosupremolecular gels which show reversible mechanoresponsive sol–gel transitions on shaking, heating or addition of acid were prepared. The cross-linked metallosupramolecular gel structure was achieved by the combination of Zn^{II} or Co^{II} ions coordinated to the 2,6-bis(1′-methylbenzimidazolyl)-pyridine (MeBIP) functionalized monomer with a ratio of 2 : 1, and the lanthanoid La^{III} or Eu^{III} ions which coordinate with the ligand with a ratio of 3 : 1 (Fig. 9a). The selective cleavage of the lanthanoid-ligand cross-linking points on application of stimuli is considered to be the cause of the collapse of the gel structure, leading to the sol–gel transition. At the same time, in the case of the Eu^{III} containing gel, a decrease of the lanthanide-based emission is observed. The thixotropic behavior of the Zn/La gel is shown in Fig. 9b, where the original gel structure could be restored after *ca.* 20 seconds of standing.

Similar mechanoresponsive sol–gel transition or thixotropy in metallosupramolecular gel systems has been reported involving various metals such as Rh,[40] Ir,[40] Eu,[41] Tb[41] and Cd.[42]

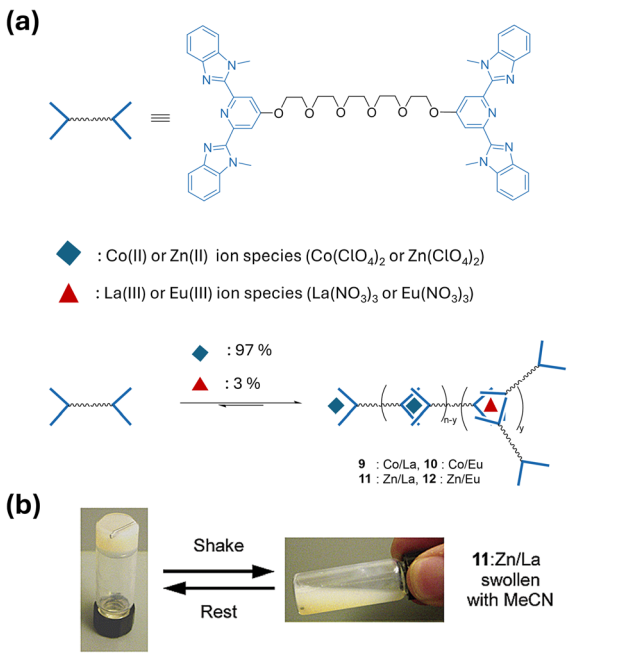

Fig. 9 (a) A schematic representation of the formation of metallosupramolecular gel-like materials using a combination of lanthanoid and transition metal ions mixed with the telechelic monomer. (b) The mechanoresponse of the Zn/La gel. Image (b) is adapted with permission from ref. 16*a*. Copyright 2003, American Chemical Society.

Some examples, in particular those involving lanthanide ions, tend to form photoluminescent gels, and their emission properties can also be altered *via* the mechano-induced sol–gel transition.[41]

The utilization of labile, photoluminescent Eu complexes to observe mechano-induced changes in polymers was reported by Weder and co-workers in 2014.[43] They prepared a crosslinked metallopolymer consisting of Eu^{III} and MeBIP functionalized poly(ethylene-*co*-butylene) telechelic chains (BKB) (Fig. 10a and b), which showed a decrease of Eu^{III} based red emission on ultrasonication of the solution (Fig. 10c). Furthermore, the solid films can show mechano-induced self-healing properties: pushing together the cut films under ultrasonication resulted in welding the films together, with their original mechanical properties fully restored. Finally, application of the mechanical force to the films after treating them with a $Fe(ClO_4)_2$ salt induced a visible color change from colorless to purple *via* the metal-exchange reaction (Fig. 10d). However in this case, the color change is irreversible due to the stronger binding of the Fe^{2+} ions with the ligand.

Furthermore, in 2018, He and co-workers reported multi-stimuli responsive luminescence changes in Eu^{3+}-containing hydrogels (Fig. 11).[44] The Eu^{3+}-containing hydrogels were prepared by addition of $Eu(NO_3)_3$ to an aqueous solution of the hydrophilic polymer P(DMA_{290}-*co*-$IDHPMA_{96}$) bearing iminodiacetate (IDA) coordination sites, to form an Eu-crosslinked network. The strongly red-emissive hydrogel showed a stimuli-induced sol–gel transition accompanied by a decrease in red emission after the addition of acid, increase of temperature, or ultrasonication. In all cases after restoring the environment to the original state gels were reformed and the emission from the Eu^{3+}–IDA was also restored. Moreover, the compression of a hydrogel consisting of a strong interpenetrating polymer network of P(DMA_{290}-*co*-$IDHPMA_{96}$) and poly(acrylic acid) showed a reversible transition from emissive to an opaque, non-emissive state.

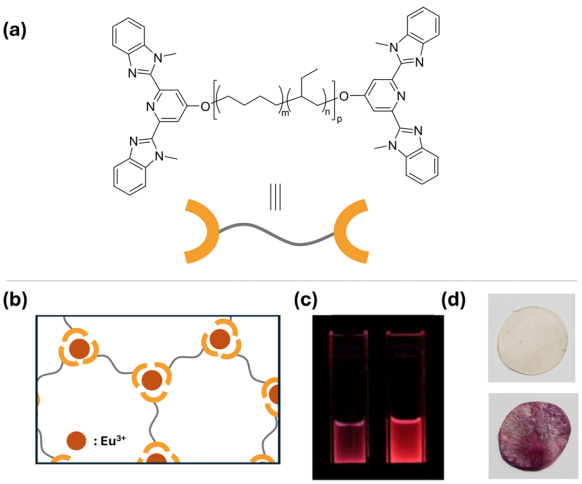

Fig. 10 (a) Structure of the BKB telechelic ligand. (b) Schematic illustration of the Eu^{3+}–BKB metallosupramolecular networks. (c) Picture cuvettes containing a solution of $[Eu(BKB)_{1.5}](ClO_4)_3$ before (right) and after ultrasonication (under UV). (d) Pictures of $[Eu(BKB)_{1.5}](ClO_4)_3$ films before treatment (top) and after swelling in a solution of $Fe(ClO_4)_2$ and subsequently ultrasonicating in CH_3CN (bottom). Images (c) and (d) are adapted with permission from ref. 43. Copyright 2014, American Chemical Society.

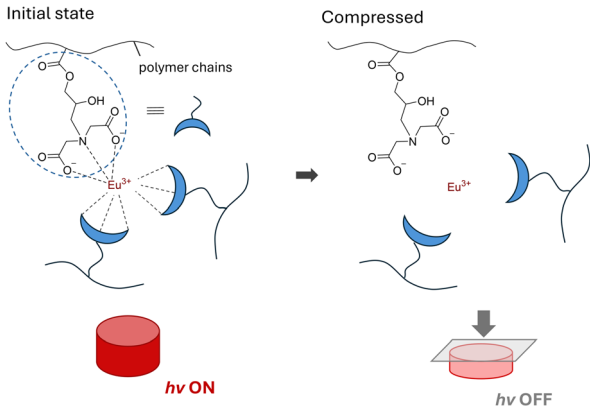

Fig. 11 Schematic illustration of the compression induced luminescence change of hydrogels containing EU^{3+}–IDA complexes. Figure redrawn from ref. 44.

A detailed experimental study on the effect of different metals on the properties of the polymers with dynamic coordination bonds was reported by Tew and co-workers in 2022.[45] In the polymer network cross-linked with metal–terpyridine (Tpy) complexes, a clear trend was observed where the stress relaxation time followed the order of $RuCl_2$ > $FeCl_2$ > $NiCl_2$ > $CoCl_2$ > $ZnCl_2$ > $MnCl_2$, which is consistent with the relative stability of M^{II}–Tpy bonds reported in previous literature.[46] The effect of the counteranions was also studied in this work, where the networks with acetate showed faster stress relaxation in general. This is consistent with the previous work by Bao and co-workers, where coordination networks bearing non-coordinating triflate anions showed superior mechanical properties compared to the samples with strongly coordinating nitrate anions.[47]

Coordination of a π-system to a late transition metal has also been exploited as a mechanoresponsive motif in polymers. Diesendruck and co-workers reported that when Rh_2Cl_2–π bridges are introduced into the polybutadiene-based single-chain polymer nanoparticles, the weaker Rh–π coordination bonds can be cleaved preferentially under ultrasonication, preventing the degradation of the molecular weight of the chain. These polymer nanoparticles could also thermally refold once the stress was removed.[48]

A potential practical utilization of the dynamic coordination mechanoresponsive systems is the stimuli-triggered cargo-release, which can be used for drug delivery and other applications. In 2014, Xia and co-workers reported opening up metallosupramolecular block copolymer micelles of Cu^{II} and Tpy modified polymers (PPG–[Cu]–PEG, Fig. 12a) to release small molecules on application of high intensity focused ultrasound (HIFU) (Fig. 12b).[49] The release of the cargo was monitored by employing fluorescent cargo molecules which are quenched upon release. Reversible reassembly of the micelles can be observed after termination of HIFU. In the control experiments, Ru^{II} analogue micelles PPG–[Ru]–PEG with a strong coordination bond and PEO–PPO–PEO with a

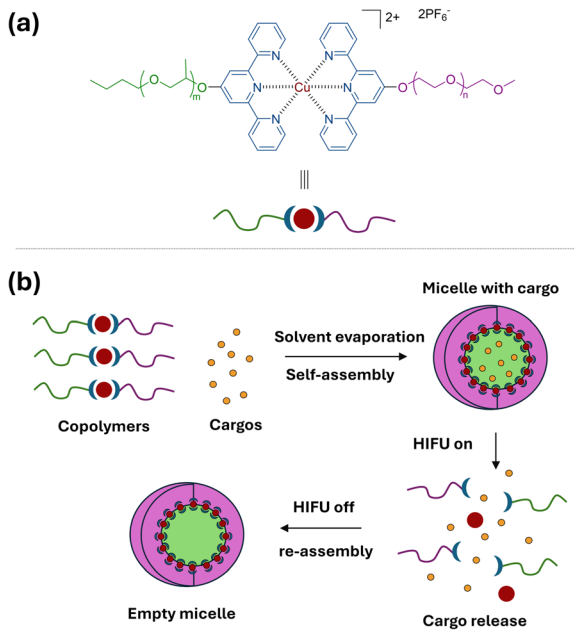

Fig. 12 (a) Structure of the PPG–[Cu]–PEG block copolymer. (b) Schematic illustration of the HIFU responsive process of block copolymer micelles containing labile Cu^{II}–Tpy bonds. Figure redrawn from ref. 49.

covalent bond were subjected to HIFU power of 2 and 7 W, with no cargo release being observed after 30 min. On the other hand, in the case of the PPG–[Cu]–PEG micelle, the released percentage of the cargo reached ~75% in 30 min at a HIFU power output of 2 W, demonstrating the lability of the Cu^{II}–Tpy bond compared to the Ru^{II}–Tpy coordination bond or covalent bonds.

Bettinger and co-workers have also investigated ultrasound-responsive Fe^{III}-containing hydrogels, which can be potentially used for biomedical applications. By varying the ratio of Fe^{III} species and the dopamine moieties in the system, hydrogels showing different mechanical, sonolysis, and self-healing properties were prepared.[50]

Interaction of metal species with organic mechanophores

So far we have discussed the mechanoresponsive polymer systems where metal complexes themselves act as mechanophores. In this section, we will introduce examples where the interaction of metal species in the polymers incorporating well-known organic mechanophores can alter or improve their properties in comparison with conventional, non-metal containing systems.

In 2013, Hong *et al.* have prepared polyurethane films showing both mechanochromism by the spiropyran (SP) mechanophore and self-healing properties by dynamic metal–ligand coordination.[51] The metallo-supramolecular gels were prepared by polymerization of 2,6-bis(1,2,3-triazol-4-yl)pyridine (BTP) ligands and SP moieties, followed by the addition of Zn^{II} or Eu^{III} species, where Zn ions form 2 : 1 ligand : metal complexes and Eu ions form 3 : 1 complexes (Fig. 13a). When compared to the control film which does not contain metal ions, a significant increase of the tensile properties such as strain at breaking was observed in both Zn- and Eu-containing films owing to metallo-supramolecular interactions. Incorporation of the metal species also shifted the color of the films after rupture to red as opposed to purple for the control films (Fig. 13b), which is attributed to binding of the dissociated parts of complexes to the merocyanine (MC) form of SP. The Zn^{II} incorporating films showed good self-healing properties with the mechanical properties of the film restored after treatment, while in the case of Eu^{III} films, healing was less efficient. This is considered to be due to the high chain branching and less chain mobility/flexibility of the Eu incorporating polymer, as well as the effect of the lower concentration of Eu species compared to Zn.

Another recent example by Braun and co-workers clearly shows the interaction between the metal ions dispersed in the polymer and the MC formed by ring-opening of SP (Fig. 14a).[52] Li^+, Ca^{2+} or Mg^{2+} salts were introduced into polydimethylsiloxane films incorporating SP mechanophores and the color

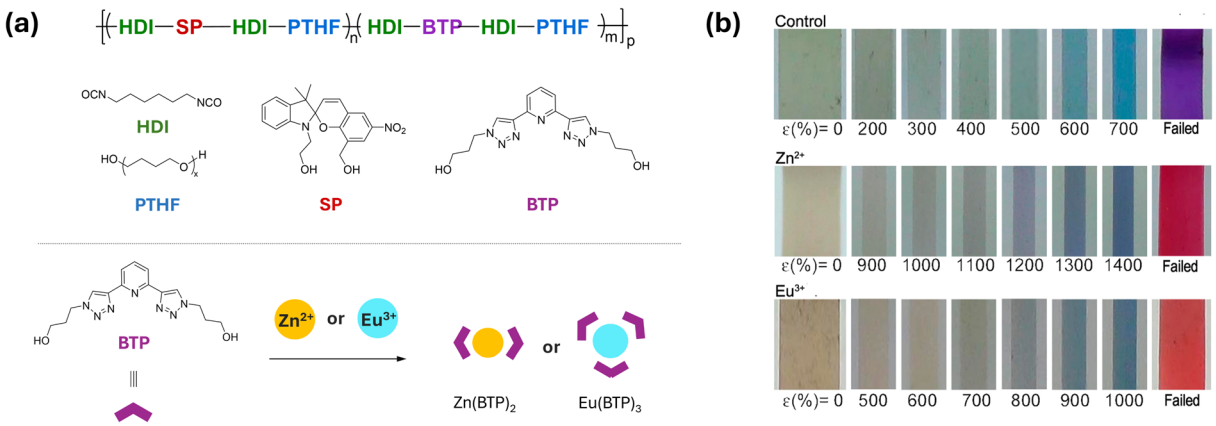

Fig. 13 (a) Structure of PU films incorporating SP and BTP ligands, and the coordination of BTP ligands to Zn^{2+} and Eu^{3+} ions. (b) Mechanically induced color change of the control film (without metal species) and the metallosupramolecular films (incorporating Zn^{2+} or Eu^{3+} ions) at variable strain ε (%). Image (b) is reproduced with permission from ref. 51. Copyright 2013, American Chemical Society.

change of the films by MC–metal bond formation was monitored by measuring the UV/vis absorbance. Under dark conditions, the films show spontaneous coloration due to the equilibrium between the ring-closed SP and metal-coordinated MC even before application of force. This degree of spontaneous coloration before stretching ($A_{thermal}$) is affected by multiple factors such as the solvent, electron-withdrawing substituents on the SP, and the metal ions. It was found that when spontaneous activation is present at a certain degree, the efficiency of activation by mechanical force ($A_{mechanical}/A_{thermal}$) becomes sensitive to $A_{thermal}$. At this point, differences in the coordination strength among different metals which result in different $A_{thermal}$ have a clear effect on mechanical activation efficiency. As a result, the weakly coordinating Li^+ showed the highest contrast in color before and after stretching (Fig. 14b).

Yang *et al.* demonstrated that by the covalent incorporation of the [Eu(2-thenoyltrifluoroacetone)$_3$(1,10-phenanthroline)] complex (Eu(TTA)$_3$(Aphen)) into the side chain of a 1,2-dioxetane cross-linked PMA, it is possible to turn the blue chemiluminescence from cleaved dioxetane to a narrow and intense red emission band from the Eu^{III} center (Fig. 15).[53] Red emissive materials are of high interest due to their potential applications in sensors, bioimaging, and light emitting diodes with advantages of low energy, strong penetrability, and high resolution. However, examples of mechanoresponsive polymer systems emitting in red or near-IR region remain limited. In this work, the energy transfer from the cleaved bis(adamantyl)-1,2-dioxetane to the Eu(TTA)$_3$(Aphen) moiety within the polymer leads to the sharp red emission at 613 nm from transparent films, corresponding to the $^5D_0$ $^7F_2$ transition of Eu^{III} ions. A control experiment where the non-bound Eu^{III} complex was dispersed in the polymer, resulted in aggregation and less intense mechanoluminescence, highlighting the advantages of covalently linking the mechanophores.

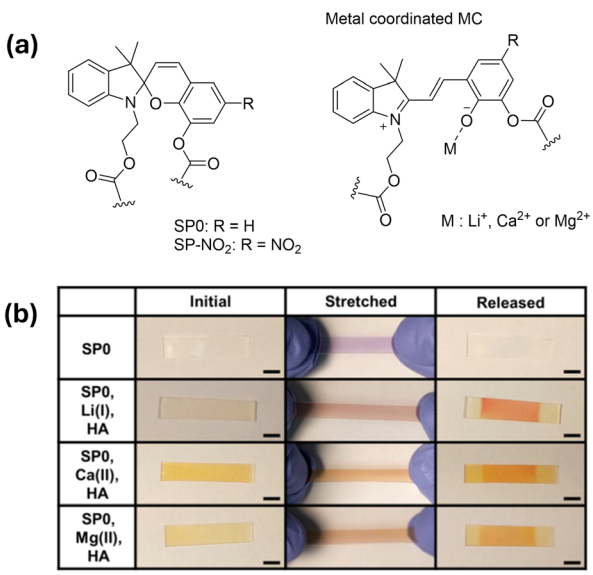

Fig. 14 (a) Structures of SP derivatives incorporated in polydimethylsiloxane and their metal-coordinated MC form. (b) Photographs of polymer films incorporating SP0, hexyl acetate and various metal salts before stretching, after stretching and immediately after releasing the films. Image (b) is reproduced with permission from ref. 52. Copyright 2020, American Chemical Society.

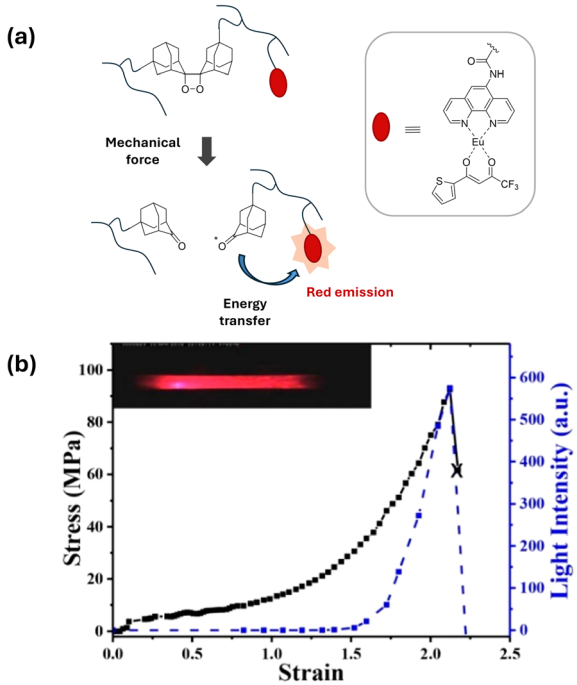

Fig. 15 (a) Schematic illustration of the bis(adamantyl)-1,2-dioxetane cross-linked PMA incorporating (Eu(TTA)$_3$(Aphen)) complexes, and the mechanically induced chemiluminescence through energy transfer. (b) Changes of stress and light intensity against strain upon stretching the film (the inset shows a picture of the film before fracture). Image (b) is reproduced with permission from ref. 53. Copyright 2020, American Chemical Society.

Metal complexes with conformationally labile ligands

In many examples discussed above, mechanoactivation of metal complexes is based on the cleavage of a metal–ligand bond (reversible or irreversible), leading to the cleavage of the polymer chain or a cross-linker. Alternatively, the ability to control mechanoresponsive properties *via* more subtle, non-destructive conformational changes or non-covalent interactions has garnered recent attention. In particular, Sagara and Weder have developed rotaxane-based mechanophores, which show a reversible response based on the association/dissociation of the weakly interacting fluorophore/quencher pair.[10a,c] Furthermore, Kotani *et al.* recently reported a photoluminescent mechanoprobe based on a conformationally flexible conjugated small molecule, which shows emission at different wavelengths in the bent and straightened states.[11c] This "flapping molecule", when incorporated into polymer chains, can be excited by mechanical force, changing the distribution between the two forms and allowing for the monitoring of force distribution in bulk material reversibly and in real time.

Conformationally fluxional metal complexes, often supported by large macrocyclic ligands, offer an interesting and

underexplored motif in the design of mechanophores. The ligand, typically a large macrocycle, may be attached to the polymer chains through the weakly coordinated atoms or other fragments that may be responsive to mechanical force applied to the polymer sample. This occurs through mechanical force resulting in a restriction of the conformational changes in the ligand, affecting the coordination environment around the metal, without leading to polymer chain or cross-linker bond scission.

Based on our group's longstanding interest in studying conformational behavior of metal complexes, we first proposed to use complexes supported by a tetradentate pyridinophane ligand (N4) attached to the polymer matrix. The previous studies of pyridinophane complexes revealed their rich conformational behavior in solution, where the N4 may coordinate in a bidentate, tridentate, or a tetradentate fashion to a metal center, showing fluxional behavior in solution (Fig. 16).[54]

In order to achieve a detectable response in a polymer-supported system, copper(I) pyridinophane complexes were selected as they are photoluminescent in solution and in the solid state. The photoluminescence quantum yield in copper complexes has previously been reported to be dependent on the conformational lability or the coordination of external ligands. In the case of copper(I) pyridinophane complexes, we have also shown that the photoluminescence quantum yield (PLQY) increases in less fluxional complexes.[54d,55]

As conformational changes in such complexes (see below) often involve changes in coordination of the pendant amine group, the amine substituents were selected as the main target for the covalent attachment of N4 to the polymer chain.

In our first reports, a hydroxy-functionalized ligand was incorporated as a part of the linear polyurethane chain and further metalated with copper(I) iodide.[56] The resulting samples showed an increase in photoluminescence intensity in response to tensile stretching observed at a millisecond time scale.

The drawback of the initial system was a relatively low PLQY of copper iodide complexes, their sensitivity to air, and the significant strain required to observe measurable changes in photoluminescence intensity. To overcome these challenges and obtain more robust and sensitive mechanophores, our group then utilized a series of pyridinophane $(N4)Cu(NHC)^+$ mechanopores used as cross-linkers in poly(butyl acrylate) samples (Fig. 17).[55] These complexes showed greater stability in air and allowed us to obtain fast and reversible changes in response to mechanical stretching even at small strain ($<50\%$) and stress (<0.1 MPa) values. Control experiments by physical blending of the model complex into the polymer film showed no noticeable increase in photoluminescence intensity, suggesting that covalent attachment was necessary for the response.

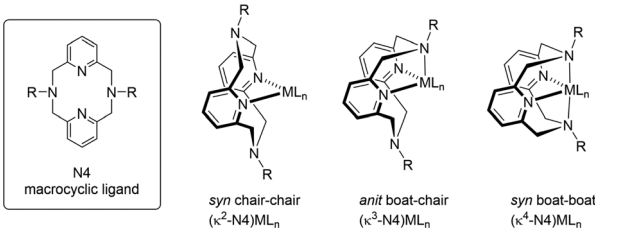

Fig. 16 Structure of the N4 macrocyclic ligand and the coordination modes of N4 in metal complexes.

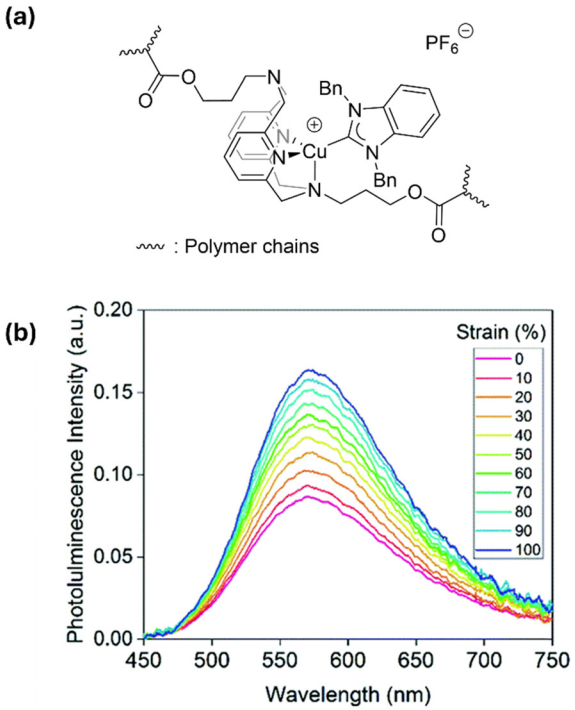

Fig. 17 (a) Structure of the N4–Cu–NHC complex incorporated into PBA chains. (b) Emission spectra of the PBA film incorporating the N4–Cu–NHC complex during stretching from 0% to 100%. Image (b) is reproduced with permission from ref. 55. Copyright 2020, The Royal Society of Chemistry.

An empirical study of the photophysical properties of the model Cu–NHC complexes revealed that the complexes bearing bulkier substituents (*e.g.* ^{t}Bu groups) on the bridging amines show less fluxionality, and thus a slower conformational exchange between the κ^3 coordination mode and the κ^4 mode in solution, compared to complexes bearing less bulky substituents. Complexes bearing bulkier substituents also displayed a trend of an increase in PLQY and a decrease of the non-radiative decay constant k_{nr} in solution. Based on these observations and the literature reports on other emissive Cu^I complexes, we proposed that the mechanism of the increase in emission intensity on application of force through polymer chains to the bridging amines is the restriction of the fluxionality of the complexes and suppression of the Jahn–Teller distortion in the excited state which promotes the non-radiative decay. Furthermore, suppression of the formation of the exciplex by coordination of the pendant amine of the N4 ligand may also be responsible for the increase in PLQY.

Filonenko and co-workers have also demonstrated the use of $(N4)Cu(NHC)^+$ complexes with a *N*,*N*′-dimethylimidazolium derived NHC ligand for the study of the deformation behavior of the different phases of PU on stretching.[57] Later the same group reported the mechanochromism of the analogous $N4–Cu^I–NHC$ mechanophores in the PU soft phase on tensile

stretching, attributed to the anion–cation separation which occurs as the result of the free volume increase of the polymer on elongation.[58]

All abovementioned (N4)Cu complexes showed emission in the range of *ca.* 560–585 nm, affected by the ligand environment around the Cu center. Taking this into account, we aimed to shift the emission of copper complexes to near-IR or red region because of the high permeability and low scattering rate that may find applications such as bioimaging, or imaging in other non-transparent materials which otherwise absorb visible light.

Examples of efficient, red-emitting Cu complexes are not very common in the literature despite the practical interest in developing efficient red emitters based on inexpensive metals.

We were able to obtain a new family of red-emitting Cu complexes based on pyridinophane and an amide ligand that show emission maxima at a λ_{max} of 598–745 nm in the crystalline state and in solution (Fig. 18a).[59] TD-DFT studies suggested that the shift in absorption can be attributed to ligand-to-ligand charge transfer from the highest occupied molecular orbital (HOMO) localized on the carbazole ligand to the lowest unoccupied molecular orbital (LUMO) localized on the N4 ligand.

Accordingly, using electron-donating substituents in the carbazolate ligand was used a tool to induce a red shift by reducing the HOMO–LUMO gap.

These complexes were covalently incorporated as cross-linkers into poly(butyl acrylate) samples, which showed a sensitive and reversible increase in PL intensity in response to mechanical stretching, repeatable over 30 cycles. The changes in PL intensity could be detected spectroscopically or with a CCD camera (Fig. 18b–d).

We have investigated the conformational behaviour of (N4)Cu complexes experimentally and by DFT calculations.[54d,55,59] In solution, the major NMR peaks of the N4–Cu–amide complexes are attributed to the κ^3 isomer; however in the case of some complexes, small peaks attributed to the minor κ^4 isomer could be also observed. Also, some peaks of the pyridinophane ligand of the κ^3 isomer show broadening, indicating a generative exchange between the two κ^3 isomer forms (Fig. 19a). According to the calculated energy profile of complex **13**, the exchange occurs through the associative pathway through κ^4-**13**, rather than the dissociative pathway involving the κ^2-**13** (Fig. 19b). The activation barrier of 15.0 kcal mol^{-1} is easily accessible at room temperature. The small difference in energies between κ^3-**13** and κ^4-**13** (1.6 kcal mol^{-1}) is also consistent with the NMR evidence for the presence of the κ^4-**13** complex as the minor isomer in solution.

Summary and future outlook

In this article, we have covered several classes of coordination compounds used as versatile and convenient mechanophores in polymers, with uses ranging from inducing mechanoactivated catalysis, to changes in color, mechanical, or photoluminescence properties. The representative examples of mechanoresponsive polymers incorporating metal complex-

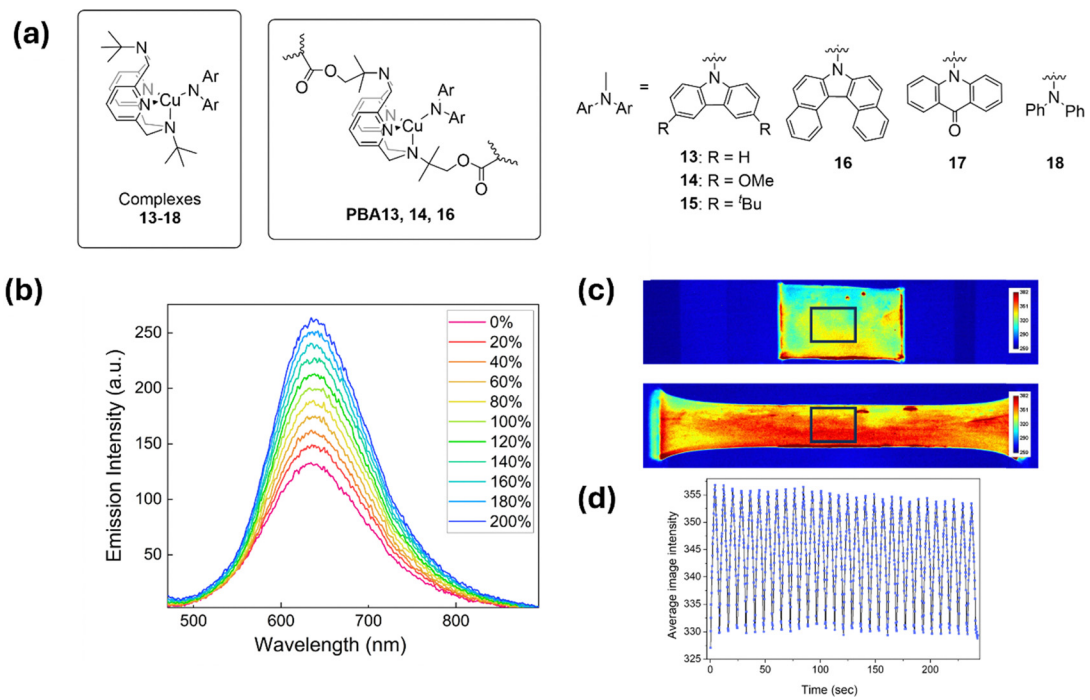

Fig. 18 (a) Structure of the model N4–Cu–amide complexes **13–18** and the N4–Cu–amide complexes incorporated in PBA chains. (b) Photoluminescence spectra of film **PBA16** during stepwise stretching from 0% to 200% strain. (c) Optical imaging of film **PBA13** at 0% (top) and 200% (bottom) strain (in pseudocolor based on grayscale pixel intensity). (d) Change of average image intensity of the selected area of the film (black square of (c)) during 30 cycles of continuous stretching and releasing (0%–200%–0%) measured with a CCD camera. Images (b)–(d) are reproduced with permission from ref. 59. Copyright 2024, The Royal Society of Chemistry.

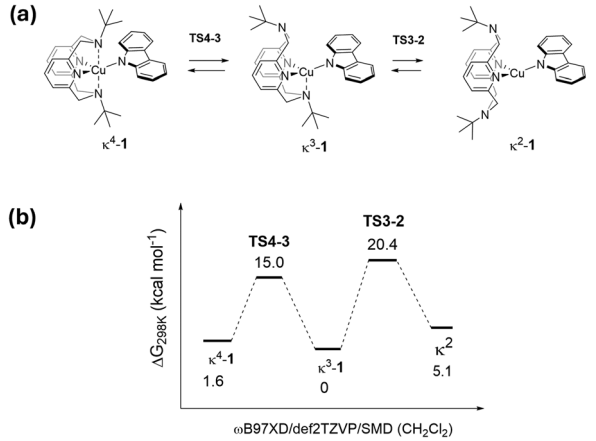

Fig. 19 (a) Proposed mechanism of the generative exchange between the two κ^3 isomers of complex **13** in solution. (b) Calculated energy profile of the isomerization of complex **13** in CH_2Cl_2.

based mechanophores highlighted in this paper are summarized in Table 1.

One strategy to activate metal complexes used as mechanophores is based on an irreversible bond cleavage, for example, in metal–N-heterocyclic carbene complexes leading to the rupture of the polymer chain and the generation of the catalytically active species by mechanical action on a bulk sample or ultrasonication of a polymer solution.

In another approach, metallocenes were used as robust and simple mechanophores that are cleaved by mechanoactivation, usually in an irreversible manner, leading to metal ion release and changes in the properties of the bulk sample (for example: color).

An alternative strategy relies on the use of labile coordination compounds *via* dynamic and reversible metal–ligand bond dissociation, which results in change of the rheological or/and photophysical properties of the materials. Furthermore, dynamic coordination systems found applications in the design of cargo-release systems.

Another approach of the application of coordination chemistry in mechanoresponsive polymers is their combination with organic mechanophores. The presence of metal ions or metal complexes in the system can alter its mechanoresponsive properties by the interactions of the metal species with the activated mechanophore resulting in a different response from their counterparts solely incorporating the organic mechanophore such as the shift in the color of the mechanochromism or the emission wavelength.

Finally, using the polymer-attached conformationally labile ligand and their copper complexes avoids the irreversible release of the metal and leads to fast and reversible changes in the photoluminescence properties of the polymer sample upon mechanical activation.

Overall, the use of coordination compounds has significantly expanded the library of existing mechanophores, which have a number of features that make them complementary to the classical organic-based mechanophores such as spiropyran. In particular, the metal–ligand bond strength can be adjusted by choosing the needed metal–ligand combination. Depending on the system, reversible dissociation of the ligand can be conveniently achieved, a phenomenon which is less common in organic mechanophores where covalent bonds often have to be cleaved. Metal complexes allow for an easier modulation of their spectroscopic or photoluminescence properties *via* altering ligand substituents or changing a spectator ligand. This allows for a custom-design of metal-based mechanophores, where ultimately efficient red emitters based on inexpensive metals using relatively simple ligand motifs can be obtained. Mechanoactivation of metal complexes can also provide important information about the nature of metal–ligand bonds and the interplay between the macroscopic properties of a material, and molecular changes around the metal center. The major challenges towards wider utilization of mechanophores based on metal complexes are often related to their stability or air sensitivity and biocompatibility, as well as the high cost in the case of precious metals. Therefore, the exploration of air-stable,

Table 1 Overview of representative examples of mechanoresponsive polymers containing metal complexes as mechanophores

Mechanophore	Activation method	Response	Ref.
Ag^{I}–NHC, Ru^{II}–NHC	Ultrasonication	RCM, ROMP reaction	18
Ru^{II}–NHC	Compression	ROMP reaction	21
Cu^{I}–NHC	Ultrasonication, compression	CuAAC reaction	22
Pt–acetylide	Ultrasonication	Olefin hydrosilylation reaction	29
Fc	Ultrasonication	Release of iron ion	33
Fc	Ultrasonication	Release of iron ion	34
Ruthenocene	Ultrasonication	Cleavage of ruthenocene	35*a*
Cobaltocenium	Ultrasonication	Cleavage of cobaltocenium	35*b*
Fc	Ultrasonication, drop test, pressure bar test	Release of iron ion, cross-linking	36
[Zn^{II} or Co^{II}/La^{III} or Eu^{III}]–MeBIP	Shearing (shaking)	Sol–gel transition, emission intensity change	16*a*
Eu^{III}–MeBIP	Ultrasonication, piercing	Emission intensity change, welding, color change	43
Eu^{III}–IDA	Ultrasonication, compression	Emission intensity change	44
Cu^{II}–Tpy	HIFU	Cargo release	49
Zn^{II}, Eu^{III}–BTP/Sp	Stretching	Color change	51
Li^{I}, Ca^{II}, Mg^{II}/Sp	Stretching	Color change	52
[$Eu^{III}(TTA)_3$(Aphen)]/1,2-dioxetane	Stretching	Light emission	53
N4–Cu^{I}–NHC	Stretching	Emission intensity change	55
N4–Cu^{I}–arylamide	Stretching	Emission intensity change	59

non-toxic and cost-effective metal complex-based mechanophores represents a promising direction for future research.

Author contributions

T. G. analyzed the literature and wrote the first draft of the manuscript. J. K. and T. G. discussed and edited the manuscript.

Data availability

No primary research results, software or code have been included and no new data were generated or analyzed as part of this review.

Conflicts of interest

There are no conflicts to declare.

Acknowledgements

We would like to thank Dr E. Khaskin for helpful suggestions on the manuscript writing.

Notes and references

1 (*a*) J. Li, C. Nagamani and J. S. Moore, *Acc. Chem. Res.*, 2015, **48**, 2181–2190; (*b*) Y. Chen, G. Mellot, D. van Luijk, C. Creton and R. P. Sijbesma, *Chem. Soc. Rev.*, 2021, **50**, 4100–4140; (*c*) H. Traeger, D. J. Kiebala, C. Weder and S. Schrettl, *Macromol. Rapid Commun.*, 2021, **42**, 2000573; (*d*) Y. Huang, S. Huang and Q. Li, *ChemPlusChem*, 2023, **88**, 202300213.

2 (*a*) S. L. Potisek, D. A. Davis, N. R. Sottos, S. R. White and J. S. Moore, *J. Am. Chem. Soc.*, 2007, **129**, 13808–13809; (*b*) D. A. Davis, A. Hamilton, J. Yang, L. D. Cremar, D. Van Gough, S. L. Potisek, M. T. Ong, P. V. Braun, T. J. Martinez, S. R. White, J. S. Moore and N. R. Sottos, *Nature*, 2009, **459**, 68–72; (*c*) C. K. Lee, B. A. Beiermann, M. N. Silberstein, J. Wang, J. S. Moore, N. R. Sottos and P. V. Braun, *Macromolecules*, 2013, **46**, 3746–3752; (*d*) Y. Lin, M. H. Barbee, C. C. Chang and S. L. Craig, *J. Am. Chem. Soc.*, 2018, **140**, 15969–15975.

3 (*a*) M. J. Robb, T. A. Kim, A. J. Halmes, S. R. White, N. R. Sottos and J. S. Moore, *J. Am. Chem. Soc.*, 2016, **138**, 12328–12331; (*b*) M. E. McFadden and M. J. Robb, *J. Am. Chem. Soc.*, 2019, **141**, 11388–11392; (*c*) B. A. Versaw, M. E. McFadden, C. C. Husic and M. J. Robb, *Chem. Sci.*, 2020, **11**, 4525–4530.

4 H. Qian, N. S. Purwanto, D. G. Ivanoff, A. J. Halmes, N. R. Sottos and J. S. Moore, *Chem*, 2021, **7**, 1080–1091.

5 (*a*) Y. Chen, A. J. Spiering, S. Karthikeyan, G. W. Peters, E. W. Meijer and R. P. Sijbesma, *Nat. Chem.*, 2012, **4**, 559–562; (*b*) E. Ducrot, Y. Chen, M. Bulters, R. P. Sijbesma and C. Creton, *Science*, 2014, **344**, 186–189; (*c*) Y. Chen and R. P. Sijbesma, *Macromolecules*, 2014, **47**, 3797–3805.

6 (*a*) K. Imato, A. Irie, T. Kosuge, T. Ohishi, M. Nishihara, A. Takahara and H. Otsuka, *Angew. Chem. Int. Ed.*, 2015, **54**, 6168–6172; (*b*) K. Imato, T. Kanehara, T. Ohishi, M. Nishihara, H. Yajima, M. Ito, A. Takahara and H. Otsuka, *ACS Macro Lett.*, 2015, **4**, 1307–1311.

7 (*a*) R. Göstl and R. P. Sijbesma, *Chem. Sci.*, 2016, **7**, 370–375; (*b*) H. Zhang, D. Zeng, Y. Pan, Y. Chen, Y. Ruan, Y. Xu, R. Boulatov, C. Creton and W. Weng, *Chem. Sci.*, 2019, **10**, 8367–8373; (*c*) X. Wang, Y. Cao, Y. Peng, L. Wang, W. Hou, Y. Zhou, Y. Shi, H. Huang, Y. Chen and Y. Li, *ACS Macro Lett.*, 2022, **11**, 310–316; (*d*) H.-C. Chang, M.-C. Liang, V.-S. Luc, C. Davis and C.-C. Chang, *Chem. – Asian J.*, 2024, **19**, 202300850.

8 (*a*) Z. Chen, J. A. M. Mercer, X. Zhu, J. A. H. Romaniuk, R. Pfattner, L. Cegelski, T. J. Martinez, N. Z. Burns and Y. Xia, *Science*, 2017, **357**, 475–479; (*b*) M. Horst, S. Holm, L. Valenta, T. B. Kouznetsova, J. Yang, N. Z. Burns, S. L. Craig, T. J. Martínez and Y. Xia, *J. Am. Chem. Soc.*, 2024, **146**(47), 32651–32659.

9 (*a*) J. Chen, A. W. Ziegler, B. Zhao, W. Wan and A. D. Q. Li, *Chem. Commun.*, 2017, **53**, 4993–4996; (*b*) Y. Sagara, H. Traeger, J. Li, Y. Okado, S. Schrettl, N. Tamaoki and C. Weder, *J. Am. Chem. Soc.*, 2021, **143**, 5519–5525; (*c*) H. Traeger, Y. Sagara, D. J. Kiebala, S. Schrettl and C. Weder, *Angew. Chem., Int. Ed.*, 2021, **60**, 16191–16199; (*d*) G. Zhu, T. Yu, J. Chen, R. Hu, G. Yang, Y. Zeng and Y. Li, *ACS Appl. Mater. Interfaces*, 2023, **15**, 11033–11041.

10 (*a*) Y. Sagara, M. Karman, E. Verde-Sesto, K. Matsuo, Y. Kim, N. Tamaoki and C. Weder, *J. Am. Chem. Soc.*, 2018, **140**, 1584–1587; (*b*) K. Imato, R. Yamanaka, H. Nakajima and N. Takeda, *Chem. Commun.*, 2020, **56**, 7937–7940; (*c*) T. Muramatsu, S. Shimizu, J. M. Clough, C. Weder and Y. Sagara, *ACS Appl. Mater. Interfaces*, 2023, **15**, 8502–8509.

11 (*a*) S. Ogi, K. Sugiyasu and M. Takeuchi, *Bull. Chem. Soc. Jpn.*, 2011, **84**, 40–48; (*b*) M. Raisch, W. Maftuhin, M. Walter and M. Sommer, *Nat. Commun.*, 2021, **12**, 4243; (*c*) R. Kotani, S. Yokoyama, S. Nobusue, S. Yamaguchi, A. Osuka, H. Yabu and S. Saito, *Nat. Commun.*, 2022, **13**, 303.

12 Y. Sha, Z. Zhou, M. Zhu, Z. Luo, E. Xu, X. Li and H. Yan, *Angew. Chem., Int. Ed.*, 2022, **61**, 202203169.

13 (*a*) J. N. Brantley, C. B. Bailey, J. R. Cannon, K. A. Clark, D. A. Vanden Bout, J. S. Brodbelt, A. T. Keatinge-Clay and C. W. Bielawski, *Angew. Chem., Int. Ed.*, 2014, **53**, 5088–5092; (*b*) P. Zheng, Y. Wang and H. Li, *Angew. Chem., Int. Ed.*, 2014, **53**, 14060–14063; (*c*) J. Longo, C. Yao, C. Rios, N. T. T. Chau, F. Boulmedais, J. Hemmerlé, P. Lavalle, S. M. Schiller, P. Schaaf and L. Jierry, *Chem. Commun.*, 2015, **51**, 232–235; (*d*) M. Scheurer, A. Dreuw, M. Head-Gordon and T. Stauch, *Chem. Sci.*, 2020, **11**, 6036–6044.

14 C. Rios, J. Longo, S. Zahouani, T. Garnier, C. Vogt, A. Reisch, B. Senger, F. Boulmedais, J. Hemmerlé, K. Benmlih, B. Frisch, P. Schaaf, L. Jierry and P. Lavalle, *Chem. Commun.*, 2015, **51**, 5622–5625.

15 (*a*) R. Merindol, G. Delechiave, L. Heinen, L. H. Catalani and A. Walther, *Nat. Commun.*, 2019, **10**, 528; (*b*) G. Creusen, R. S. Schmidt and A. Walther, *ACS Macro Lett.*, 2021, **10**, 671–678.

16 (*a*) J. B. Beck and S. J. Rowan, *J. Am. Chem. Soc.*, 2003, **125**, 13922–13923; (*b*) J. M. Paulusse and R. P. Sijbesma, *Angew. Chem., Int. Ed.*, 2004, **43**, 4460–4462.

17 S. Karthikeyan, S. L. Potisek, A. Piermattei and R. P. Sijbesma, *J. Am. Chem. Soc.*, 2008, **130**, 14968–14969.

18 A. Piermattei, S. Karthikeyan and R. P. Sijbesma, *Nat. Chem.*, 2009, **1**, 133–137.

19 (*a*) R. Groote, B. M. Szyja, E. A. Pidko, E. J. M. Hensen and R. P. Sijbesma, *Macromolecules*, 2011, **44**, 9187–9195; (*b*) J. Rooze, R. Groote, R. T. Jakobs, R. P. Sijbesma, M. M. van Iersel, E. V. Rebrov, J. C. Schouten and J. T. Keurentjes, *J. Phys. Chem. B*, 2011, **115**, 11038–11043.

20 R. T. M. Jakobs and R. P. Sijbesma, *Organometallics*, 2012, **31**, 2476–2481.

21 R. T. M. Jakobs, S. Ma and R. P. Sijbesma, *ACS Macro Lett.*, 2013, **2**, 613–616.

22 P. Michael and W. H. Binder, *Angew. Chem., Int. Ed.*, 2015, **54**, 13918–13922.

23 P. Michael, M. Biewend and W. H. Binder, *Macromol. Rapid Commun.*, 2018, **39**, e1800376.

24 S. Funtan, P. Michael and W. H. Binder, *Biomimetics*, 2019, **4**, 24.

25 S. Funtan, A. Funtan, R. Paschke and W. H. Binder, *Org. Mater.*, 2020, **2**, 116–128.

26 M. Biewend, P. Michael and W. H. Binder, *Soft Matter*, 2020, **16**, 1137–1141.

27 (*a*) K. S. Shinde, P. Michael, D. Fuhrmann and W. H. Binder, *Macromol. Chem. Phys.*, 2023, **224**, 2200207; (*b*) K. S. Shinde, P. Michael and W. H. Binder, *Macromol. Chem. Phys.*, 2023, **224**, 2300297.

28 H. Rupp and W. H. Binder, *Macromol. Rapid Commun.*, 2021, **42**, 2000450.

29 K. Wei, Z. Gao, H. Liu, X. Wu, F. Wang and H. Xu, *ACS Macro Lett.*, 2017, **6**, 1146–1150.

30 (*a*) T. J. Kealy and P. L. Pauson, *Nature*, 1951, **168**, 1039–1040; (*b*) D. Astruc, *Eur. J. Inorg. Chem.*, 2016, 6–29.

31 K. E. Lewis and G. P. Smith, *J. Am. Chem. Soc.*, 1984, **106**, 4650–4651.

32 Y. Sha, H. Zhang, Z. Zhou and Z. Luo, *Polym. Chem.*, 2021, **12**, 2509–2521.

33 M. Di Giannantonio, M. A. Ayer, E. Verde-Sesto, M. Lattuada, C. Weder and K. M. Fromm, *Angew. Chem., Int. Ed.*, 2018, **57**, 11445–11450.

34 Y. Sha, Y. Zhang, E. Xu, Z. Wang, T. Zhu, S. L. Craig and C. Tang, *ACS Macro Lett.*, 2018, **7**, 1174–1179.

35 (*a*) Y. Sha, Y. Zhang, E. Xu, C. W. McAlister, T. Zhu, S. L. Craig and C. Tang, *Chem. Sci.*, 2019, **10**, 4959–4965; (*b*) Y. Cha, T. Zhu, Y. Sha, H. Lin, J. Hwang, M. Seraydarian, S. L. Craig and C. Tang, *J. Am. Chem. Soc.*, 2021, **143**, 11871–11878.
36 Y. Zhang, Z. Wang, T. B. Kouznetsova, Y. Sha, E. Xu, L. Shannahan, M. Fermen-Coker, Y. Lin, C. Tang and S. L. Craig, *Nat. Chem.*, 2021, **13**, 56–62.
37 R. Dobrawa and F. Würthner, *J. Polym. Sci., Part A: Polym. Chem.*, 2005, **43**, 4981–4995.
38 (*a*) G. R. Whittell, M. D. Hager, U. S. Schubert and I. Manners, *Nat. Mater.*, 2011, **10**, 176–188; (*b*) M. Mauro, *Eur. J. Inorg. Chem.*, 2018, 2090–2100.
39 Y. Chujo, K. Sada and T. Saegusa, *Macromolecules*, 1993, **26**, 6320–6323.
40 J. M. J. Paulusse, D. J. M. van Beek and R. P. Sijbesma, *J. Am. Chem. Soc.*, 2007, **129**, 2392–2397.
41 (*a*) P. Chen, Q. Li, S. Grindy and N. Holten-Andersen, *J. Am. Chem. Soc.*, 2015, **137**, 11590–11593; (*b*) P. Sutar and T. K. Maji, *Inorg. Chem.*, 2017, **56**, 9417–9425.
42 V. K. Pandey, M. K. Dixit, S. Manneville, C. Bucher and M. Dubey, *J. Mater. Chem. A*, 2017, **5**, 6211–6218.
43 D. W. Balkenende, S. Coulibaly, S. Balog, Y. C. Simon, G. L. Fiore and C. Weder, *J. Am. Chem. Soc.*, 2014, **136**, 10493–10498.
44 G. Weng, S. Thanneeru and J. He, *Adv. Mater.*, 2018, **30**, 1706526.
45 I. Sacligil, C. W. Barney, A. J. Crosby and G. N. Tew, *Soft Matter*, 2022, **18**, 4937–4943.
46 J. M. Ludlow Iii, Z. Guo, A. Schultz, R. Sarkar, C. N. Moorefield, C. Wesdemiotis and G. R. Newkome, *Eur. J. Inorg. Chem.*, 2015, 5662–5668.
47 Y.-L. Rao, V. Feig, X. Gu, G.-J. Nathan Wang and Z. Bao, *J. Polym. Sci., Part A: Polym. Chem.*, 2017, **55**, 3110–3116.
48 A. Levy, R. Feinstein and C. E. Diesendruck, *J. Am. Chem. Soc.*, 2019, **141**, 7256–7260.
49 B. Liang, R. Tong, Z. Wang, S. Guo and H. Xia, *Langmuir*, 2014, **30**, 9524–9532.
50 W.-C. Huang, F. Ali, J. Zhao, K. Rhee, C. Mou and C. J. Bettinger, *Biomacromolecules*, 2017, **18**, 1162–1171.
51 G. Hong, H. Zhang, Y. Lin, Y. Chen, Y. Xu, W. Weng and H. Xia, *Macromolecules*, 2013, **46**, 8649–8656.
52 E. Epstein, T. A. Kim, R. H. Kollarigowda, N. R. Sottos and P. V. Braun, *Chem. Mater.*, 2020, **32**, 3869–3878.
53 F. Yang, Y. Yuan, R. P. Sijbesma and Y. Chen, *Macromolecules*, 2020, **53**, 905–912.
54 (*a*) S. P. Meneghetti, P. J. Lutz and J. Kress, *Organometallics*, 2001, **20**, 5050–5055; (*b*) J. R. Khusnutdinova, N. P. Rath and L. M. Mirica, *Inorg. Chem.*, 2014, **53**, 13112–13129; (*c*) G. A. Filonenko, R. R. Fayzullin and J. R. Khusnutdinova, *J. Mater. Chem. C*, 2017, **5**, 1638–1645; (*d*) P. H. Patil, G. A. Filonenko, S. Lapointe, R. R. Fayzullin and J. R. Khusnutdinova, *Inorg. Chem.*, 2018, **57**, 10009–10027.
55 A. Karimata, P. H. Patil, E. Khaskin, S. Lapointe, R. R. Fayzullin, P. Stampoulis and J. R. Khusnutdinova, *Chem. Commun.*, 2020, **56**, 50–53.
56 G. A. Filonenko and J. R. Khusnutdinova, *Adv. Mater.*, 2017, 29.
57 G. A. Filonenko, J. A. M. Lugger, C. Liu, E. P. A. van Heeswijk, M. Hendrix, M. Weber, C. Muller, E. J. M. Hensen, R. P. Sijbesma and E. A. Pidko, *Angew. Chem., Int. Ed.*, 2018, **57**, 16385–16390.
58 G. A. Filonenko, D. Sun, M. Weber, C. Muller and E. A. Pidko, *J. Am. Chem. Soc.*, 2019, **141**, 9687–9692.
59 T. Gridneva, A. Karimata, R. Bansal, R. R. Fayzullin, S. Vasylevskyi, A. Bruhacs and J. R. Khusnutdinova, *Chem. Commun.*, 2023, **60**, 212–215.

